

A LATERAL FLOW-THROUGH LABEL-FREE BIOSENSOR BASED ON SILICON PHOTONICS

Yifei Wang, Md. Azahar Ali, Liang Dong, and Meng Lu
Iowa State University, Ames, Iowa 50011, USA

ABSTRACT

The optical resonances of the silicon nanopost array patterned on a silicon-on-insulator (SOI) substrate have been investigated. The fabricated device supports optical resonances in the range of 1.55 μm with a variable Q-factor depending on the angle of incidence. By sealing the device on top of the nanoposts, we demonstrated a lateral flow-through label-free biosensor built on SOI. The biosensor exhibits the refractive index sensitivity of 800 nm/RIU and the femtomolar sensitivity for detection of a breast cancer biomarker (ErbB2).

KEYWORDS: Flow-Through, Nano-Fluidics, Label-Free Biosensor, Silicon Photonics

INTRODUCTION

The rapid growth of point-of-care testing demands for biomolecule sensors with higher sensitivity and smaller size. We will present an optical biosensor that exploits silicon photonics and nanofluidic technologies to fulfill these needs. The on-chip biosensor consists of a 2D array of silicon nanoposts fabricated on a SOI substrate shown in Fig. 1(a). The 2D array of silicon nanoposts can be engineered to support optical bound states and high-Q resonance modes, like the 1D high contrast gratings [1-3]. The device can be used as a label-free optical biosensor by monitoring the biomolecule-absorption-induced change in refractive index [4]. Meanwhile, the silicon nanopost structure can be utilized to achieve a lateral flow-through sensing scheme with nanofluidic channels. The fabricated biosensor exhibited a high refractive index sensitivity of 800 nm/RIU and a femto-molar sensing limit for the detection of a breast cancer biomarker.

THEORY

Rigorous coupled wave analysis was used to design and optimize the optical characteristics of the device numerically. In order to obtain the silicon nano-post biosensor resonances near 1.55 μm wavelength, the period, grating height, and post diameter of the device were chosen as $\Lambda = 1000$ nm, $t_g = 350$ nm, and $w = 570$ nm, respectively. The photonic band diagram of the device is shown in Fig. 1(b), where an optical bound state can be identified at the resonant wavelength and angle of incidence of $\lambda_r = 1595.2$ nm and $\theta_i = 0$, respectively. Fig. 1(d) compares the reflection spectra simulated for $\theta_i = 0^\circ, 1^\circ, 2^\circ, 3^\circ, 4^\circ,$ and 5° in the left panel, indicating that the Q-factor of the resonance varies in the range of 380 to 56 depending on θ_i .

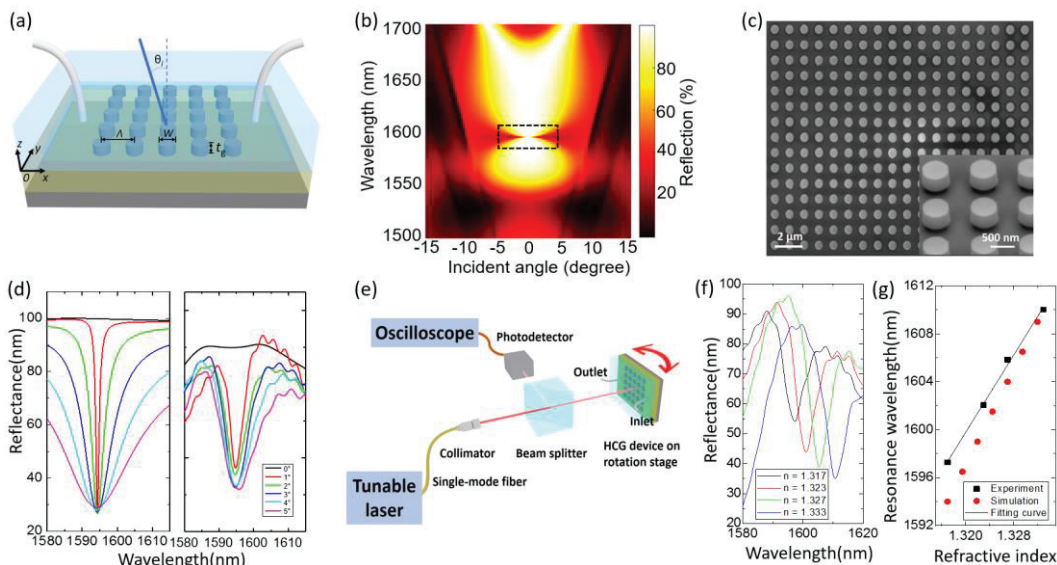


Figure 1: (a) Schematic of 2D HCG structure. (b) Calculated reflection spectra over the wavelength range 1500 to 1700 nm, and $-15^\circ < \theta_i < 15^\circ$. (c) SEM images of fabricated device. (d) Simulated (left panel) and measured (right panel) reflection spectra for $\theta = 0^\circ, 1^\circ, 2^\circ, 3^\circ, 4^\circ,$ and 5° . (e) Schematic diagram of the measurement setup. (f) Reflectance spectra measured when sensor is immersed in solutions with different refractive index. (g) Calculated and measured results of resonant wavelength versus refractive index.

EXPERIMENTAL

The array of silicon nanoposts was fabricated on a SOI substrate using e-beam lithography, evaporation, lift-off process, and deep reactive ion etching. Fig. 1(c) shows the scanning electron microscopic (SEM) images of the fabricated silicon nanoposts. The reflection measurement

setup for characterization and sensing measurement of the HCG device is shown in Fig. 1(e). The measured reflection spectra were compared to the simulated results in Fig. 1(d). The device exhibited a tunable Q-factor in the range of 250 to 130. The Fig. 1(f) shows the reflection spectra from the HCG with a 3° incident angle when its surface was immersed in ethanol/DI solutions. The resonant wavelengths are plotted as a function of refractive index in Fig. 1(g). The bulk refractive index sensitivity was calculated as $S_b = \Delta\lambda_r/\Delta n = 800 \text{ nm/RIU}$.

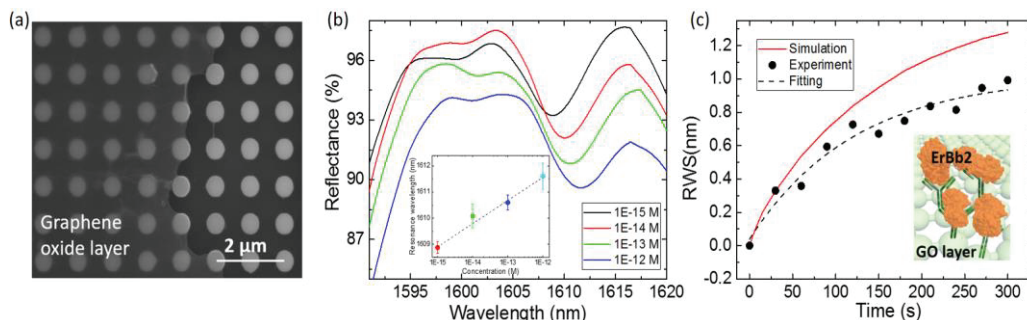


Figure 2: (a) SEM image of HCG with GO layer on the left half. (b) The reflective spectra of analyte of different concentration. Inset: the trend of resonance wavelength of the various surface concentration change. (c) The simulation (red) and experiment (black) results of dynamic binding of ErbB2 antigen. Inset: schematic of GO, anti-ErBb2 and ErBb2.

RESULTS AND DISCUSSION

To create a lateral flow-through biosensor, a polydimethylsiloxane cover was bonded to the top surface of silicon nanoposts after a 15 nm-thick graphene oxide (GO) layer was coated on sensor surface via drop casting the aqueous dispersion of GO. The capping of nanoposts forms a nanofluidic flow cell and enables analytes to laterally flow through the sensing area via the gaps created between the nanoposts.

The lateral flow-through sensor was used to detect the epidermal growth factor receptor 2 (ErbB2) proteins, a widely-used biomarker for breast cancer screening. The GO-coated nanoposts (Fig. 2(a)) were functionalized with anti-ErBb2. Fig. 2(b) shows the reflectance spectra recorded when the samples flow through the nanoposts at different analyte (ErbB2) concentrations ranging from 10^{-15} to 10^{-12} M. The inset of Fig. 2(b) gives the dose response curve for the detection, indicating a femto-molar detection limit. The device also allows the real-time monitoring of the analyte absorption. Fig. 2(c) shows the time dependent resonant wavelength shift (RWS) over a 300-sec period when 10^{-14} M concentration ErbB2 antigen flowed through the sensing area at the flow rate of 2 $\mu\text{L}/\text{sec}$. The experimental result of binding dynamics agreed well with the simulated result (Fig. 2(c)).

ACKNOWLEDGEMENTS

This work was supported by the NSF Grants ECCS-1711839, ECCS-1653673, and ECCS-0954765. Fabrication was performed in the Microelectronics Research Center at Iowa State University, as well as in the Minnesota Nanofabrication Center, which receives partial support through the National Nanotechnology.

REFERENCES

- [1] C. J. Chang-Hasnain and W. J. Yang, "High-contrast gratings for integrated optoelectronics." *Adv. Opt. Photon.* 4, 379-440 (2012).
- [2] J. W. Yoon, S. H. Song, and R. Magnusson, "Critical field enhancement of asymptotic optical bound states in the continuum." *Sci. Rep.*, 5 (2015).
- [3] Y. Wang, J. Song, L. Dong, and M. Lu, "Optical bound states in slotted high-contrast gratings." *J. Opt. Soc. Am. B* 33(12), 2472-2479 (2016).
- [4] Y. Wang, L. Dong, and M. Lu, "Optical Bound States of 2D High-Contrast Grating for Refractometric Sensing." in *CLEO, OSA*, paper JW2A.143 (2016)

CONTACT

- * M. Lu; phone: +1-515-294-9951; menglu@iastate.edu
- * L. Dong; phone: +1-515-294-0388; ldong@iastate.edu